CORE
Metadata, citation and similar papers at core.ac.uk
Provided by University of Southern Queensland ePrints

Standard Pick/Ship List

Our reference: 2365942
Your reference: 914935
Printed Date: 16-OCT-2017

Call Number:

Requested by: University of Southern Queensland
BLDSC account:

Bibliographic details
Author:
Title: Journal of Applied Physics
ISBN/ISSN: 0021-8979
Control number:
Publisher: AIP Publishing LLC
Publication Date:
Source:
Article details
Volume/Issue: 111 (10)
Article Title: Structure, piezoelectric, and ferroelectric properties of BaZrO 3 substituted Bi(Mg 1/2Ti 1/2)O 3-PbTiO 3 perovskite
Article Author: Fan, L., Chen, J., Kang, H., Liu, L., Fang, L., Deng, J., Yu, R., Xing, X.
Article Date: 2012
Pages: 104118
Items Shipped: 0

Request Notes:

FAO:
Send to:

Docstore: docs@usq.edu.au; ILL email: ills@usq.edu.au
Document Delivery, Library, University of Southern Queensland
West St
Toowoomba,, QLD
4350

Local request number:

Structure, piezoelectric, and ferroelectric properties of $BaZrO_3$ substituted $Bi(Mg_{1/2}Ti_{1/2})O_3$-$PbTiO_3$ perovskite

Longlong Fan, Jun Chen, Huajun Kang, Laijun Liu, Liang Fang, Jinxia Deng, Ranbo Yu, and Xianran Xing

Citation: Journal of Applied Physics **111**, 104118 (2012); doi: 10.1063/1.4722286
View online: http://dx.doi.org/10.1063/1.4722286
View Table of Contents: http://aip.scitation.org/toc/jap/111/10
Published by the American Institute of Physics

Articles you may be interested in

Enhanced piezoelectric and antiferroelectric properties of high-T_C perovskite of Zr-substituted $Bi(Mg_{1/2}Ti_{1/2})O_3$-$PbTiO_3$
Journal of Applied Physics **112**, 074101 (2012); 10.1063/1.4755790

Piezoelectric properties of high Curie temperature barium titanate–bismuth perovskite-type oxide system ceramics
Journal of Applied Physics **108**, 094114 (2010); 10.1063/1.3481390

Enhanced piezoelectric and ferroelectric properties in the $BaZrO_3$ substituted $BiFeO_3$-$PbTiO_3$
Applied Physics Letters **102**, 022905 (2013); 10.1063/1.4775763

Phase diagrams and electrical properties of $(Bi_{1/2}Na_{1/2})TiO_3$-based solid solutions
Journal of Applied Physics **104**, 124106 (2008); 10.1063/1.3043588

Elastocaloric effect in ferroelectric ceramics
Applied Physics Letters **106**, 172901 (2015); 10.1063/1.4919453

Temperature dependence of piezoelectric properties of high-T_C $Bi(Mg_{1/2}Ti_{1/2})O_3 - PbTiO_3$
Journal of Applied Physics **106**, 034109 (2009); 10.1063/1.3191666

Structure, piezoelectric, and ferroelectric properties of $BaZrO_3$ substituted $Bi(Mg_{1/2}Ti_{1/2})O_3$-$PbTiO_3$ perovskite

Longlong Fan,[1] Jun Chen,[1,a)] Huajun Kang,[1] Laijun Liu,[2] Liang Fang,[2] Jinxia Deng,[1] Ranbo Yu,[1] and Xianran Xing[1,3]
[1]*Department of Physical Chemistry, University of Science and Technology Beijing, Beijing 100083, China*
[2]*Key Laboratory of New Processing Technology for NonFerrous Metals and Materials, Ministry of Education, Guilin University of Technology, Guilin 541004, China*
[3]*State Key Laboratory for Advanced Metals and Materials, University of Science and Technology Beijing, Beijing 100083, China*

(Received 8 February 2012; accepted 26 April 2012; published online 30 May 2012)

The structure and electric properties of $(0.9\text{-}x)Bi(Mg_{1/2}Ti_{1/2})O_3$-$xPbTiO_3$-$0.1BaZrO_3$ ($0.45 \le x \le 0.53$) ceramics were investigated. The morphotropic phase boundary between tetragonal ferroelectric and pseudo-cubic relaxor phases is ascertained at $x = 0.50$. The $BaZrO_3$ substitution can much reduce the coercive field of $Bi(Mg_{1/2}Ti_{1/2})O_3$-$PbTiO_3$. The studies on temperature dependence of both ferroelectric and dielectric constant indicate a direct evidence for the antiferroelectric relaxor phase, which was ever suggested in the binary system of $Bi(Mg_{1/2}Ti_{1/2})O_3$-$PbTiO_3$. The phase transition of ferroelectric to antiferroelectric relaxor produces the thermal depoling below the Curie temperature. The ceramic of BMT-0.47PT-0.1BZ exhibits a high strain 0.37% and a large-signal d_{33} (530 pm/V) in the antiferroelectric-relaxor phase. $BaZrO_3$ substituted $Bi(Mg_{1/2}Ti_{1/2})O_3$-$PbTiO_3$ shows an analogous phase diagram to that of lead-free $(Bi, Na)TiO_3$-$BaTiO_3$. © *2012 American Institute of Physics*. [http://dx.doi.org/10.1063/1.4722286]

I. INTRODUCTION

Recently, the Bi-based perovskite structures $BiMeO_3$-$PbTiO_3$ solid solutions are popularly studied due to the high Curie temperature (T_C). It was ever suggested that the T_C of the compositions in the vicinity of the morphotropic phase boundary (MPB) of $BiMeO_3$-$PbTiO_3$ was linear related to the tolerance factor (t) of the end member $BiMeO_3$ compound. $BiScO_3$-$PbTiO_3$ (BS-PT) has a low t of 0.907 (Refs. 1 and 2) and exhibits an excellent high temperature piezoelectric performance. T_C at the MPB is as high as $T_C \approx 450\,^{\circ}C$ and piezoelectric parameter d_{33} is 460 pC/N. But, the utility of BS-PT is limited by the high cost of Sc_2O_3. As an analogy Bi-based compound, it is found that the $Bi(Mg_{1/2}Ti_{1/2})O_3$-$PbTiO_3$ (BMT-PT) system has a similarly high T_C (478 °C) at the MPB composition to BS-PT system, however with a relatively lower piezoelectric coefficient.[3] This may be induced by the core-shell microstructure and the oxygen octahedral rotations. The study on the temperature dependence of ferroelectric properties of BMT-PT shows that strain, remanent polarization (P_r), and the maximum polarization (P_{max}) increase with increasing temperature, and a large value of large-signal d_{33} (500 pm/V) could be obtained at high temperature. The enhanced piezoelectric property is due to the fact that domains can be easier switched with the reduced tetragonality as the temperature is raised.[4]

For the application of piezoelectric actuators, the electric field induced strain is an important parameter. The strain behavior of the piezoelectric ceramics is related to the crystal structure, domain configuration, and so on.[5–8] The antiferroelectric order can obviously enhance the strain level not only for lead but also lead-free piezoelectrics. For example, a field induced high strain could be achieved by the phase transition between antiferroelectric and ferroelectric orders in $(Pb, La)(Ti, Zr, Sn)O_3$ system.[9] As for the BMT-PT, the end member $Bi(Mg_{1/2}Ti_{1/2})O_3$, which only can be synthesized by high pressure method, is expected to be antiferroelectric structure (*Pnnm*) analogue to $PbZrO_3$. However, there is no direct polarization to manifest the order of antiferroelectric property.[10] In this study, we introduce perovskite $BaZrO_3$ into the BMT-PT system to form a ternary system. The addition of $BaZrO_3$ could reduce the tetragonality that will improve the domain mobility to raise the piezoelectric properties. Furthermore, the dielectric spectrum of Ba-based piezoelectric ceramics[11–13] exhibits that the ceramics possess relaxor character at the MPB compositions, and the dielectric loss is lower at high temperature, which could improve the resistance of piezoelectric ceramics at high temperature.

In this work, 10 mol. % $BaZrO_3$ content is added into the BMT-PT system, forming $(0.9\text{-}x)Bi(Mg_{1/2}Ti_{1/2})O_3$-$xPbTiO_3$-$0.1BaZrO_3$ (abbreviated as BMT-xPT-0.1BZ). The structure and piezoelectric and ferroelectric properties were investigated. In order to explore phase transition, the temperature dependence of dielectric and ferroelectric properties were applied. The large-signal d_{33} is much enhanced near the MPB composition. A kind of antiferroelectric-relaxor (AFE-relaxor) phase transition is also found, which contributes to the thermal depoling.

II. EXPERIMENT

The BMT-xPT-0.1BZ polycrystalline specimens were prepared by the conventional solid-state reaction method. A

a)Author to whom correspondence should be addressed. Electronic mail: junchen@ustb.edu.cn. Tel./Fax.: +86-10-62332525.

 © 2012 American Institute of Physics

stoichiometric amount of Bi_2O_3, PbO, $BaCO_3$, $4MgCO_3{\cdot}Mg(OH)_2{\cdot}5H_2O$, TiO_2, and ZrO_2 were mixed by ball mill in alcohol for 12 h. After drying, the mixed powder was calcined at 900 °C for 4 h. The calcined powder was ground and milled in ethanol again for 12 h to reduce the particle size. Then, the dried slurry was uniaxially pressed into the cylindrical pellets with a diameter of 10 mm and thickness of 3 mm with polyvinyl alcohol at a pressure of 300 MPa. The pellets were then sintered at 1150 °C for 2 h. Protective powder of the same composition was placed around the pellets to minimize the evaporation loss of PbO and Bi_2O_3 during the high temperature sintering.

The room temperature x-ray diffractometer equipped with Cu-K_α radiation was used to analyze the phase structure. The fracture microstructure of the sintered sample was examined by scanning electron microscope. The sintered pellets were grounded and polished to a thickness of ~0.6 mm and then electroded with silver paste for the measurements of electrical characteristics. The piezoelectric coefficient d_{33} was measured after poling 24 h with piezo-d_{33} meter (China Academy of Acoustics, ZJ-3). The poled samples for piezoelectric measurements were poled under a field of 70 kV/cm in silicon oil at 50 °C for 12 min. The temperature dependence of dielectric spectrum was measured on both poled and unpoled pellets using an impedance analyzer (4294 A). The polarization and longitudinal strain vs. electric field hysteretic loops were characterized by a ferroelectricity analyzer (TF Analyzer 1000) at a frequency of 1 Hz. For the measurement of the temperature dependence of polarization and strain, the temperature range was from room temperature to 160 °C with a step-length of 15 °C.

III. RESULTS AND DISCUSSION

The room temperature x-ray diffraction (XRD) patterns of powders from the crushed ceramics of BMT-xPT-0.1BZ, with $0.45 \le x \le 0.53$, are shown in Fig. 1(a). All of the samples are in the pure perovskite phase. For the composition of $x \le 0.47$, its crystal structure is pseudo-cubic where no splitting of any peaks can be detected. Since the BMT-PT system was indexed in the rhombohedral phase ($R3c$) by TEM investigation,[3] we also specify these compositions with upper $Bi(Mg_{1/2}Ti_{1/2})O_3$ content as the rhombohedral phase. Tetragonal phase (T) is observed for $x = 0.53$ as displayed by the splitting of {100} and {200} peaks. It indicates that a phase change from T to R can be detected in the range of $0.48 \le x \le 0.51$. With decreasing content of $PbTiO_3$, it is evidenced that the relatively intensity of the (200) peak of the T phase to that of R phase near $2\theta = 45°$ decreases. The MPB is around the composition of BMT-0.50PT-0.1BZ. As shown in Fig. 1(b), the electric field can induce a phase transition from the R to T from the XRD profile of the poled and unpoled BMT-0.48PT-0.1BZ ceramics. It is evidenced that {200} peaks split and the relative ratio of (002)/(200) peak intensity is strengthened in the poled ceramic of BMT-0.48PT-0.1BZ.

The fracture surface of BMT-0.48PT-0.1BZ is shown in Fig. 2, it can be found that the ceramic is well densified with an average grain size of ~4 μm.

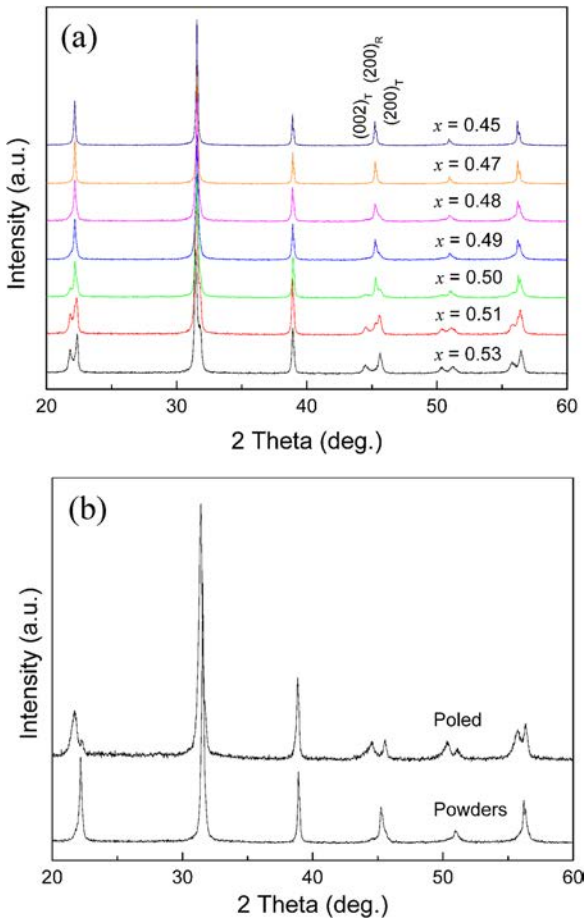

FIG. 1. (a) X-ray diffraction patterns of crushed ceramic powder of BMT-xPT-0.1BZ ($0.45 \le x \le 0.53$) at room temperature; (b) x-ray diffraction patterns of crushed ceramic powder and a poled ceramic pellet for the composition of BMT-0.48PT-0.1BZ.

For the BMT-xPT-0.1BZ ceramics with $0.45 \le x \le 0.53$, the ferroelectric hysteresis loops are shown in Fig. 3. Well saturated polarization vs. electric field, $P(E)$, loops can be obtained for the ceramics measured with an E-field of 70 kV/cm at 1 Hz. For the compositions with $x \ge 0.48$, typical $P(E)$ hysteresis loops of ferroelectric materials are shown. While the PT content decreases to $x = 0.47$, the loop

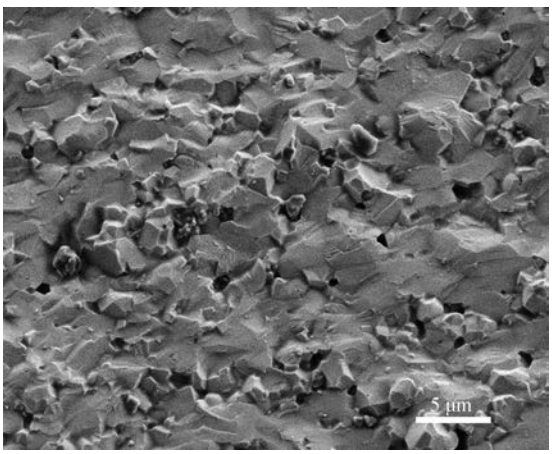

FIG. 2. Microstructure of the fracture of BMT-0.48PT-0.1BZ sintered at 1150 °C.

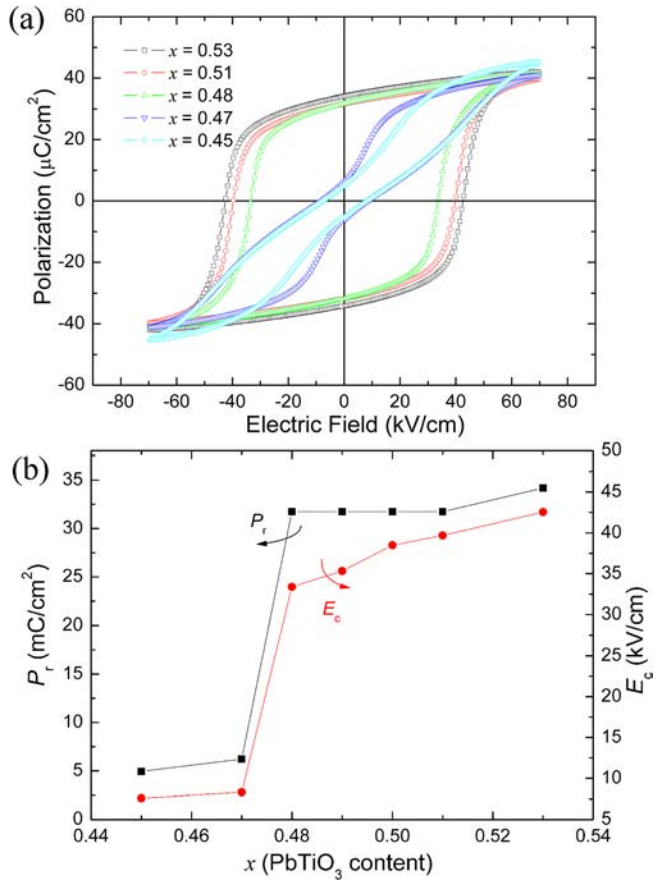

FIG. 3. (a) $P(E)$ loops and (b) P_r and E_C for the BMT-xPT-0.1BZ with $0.45 \leq x \leq 0.53$.

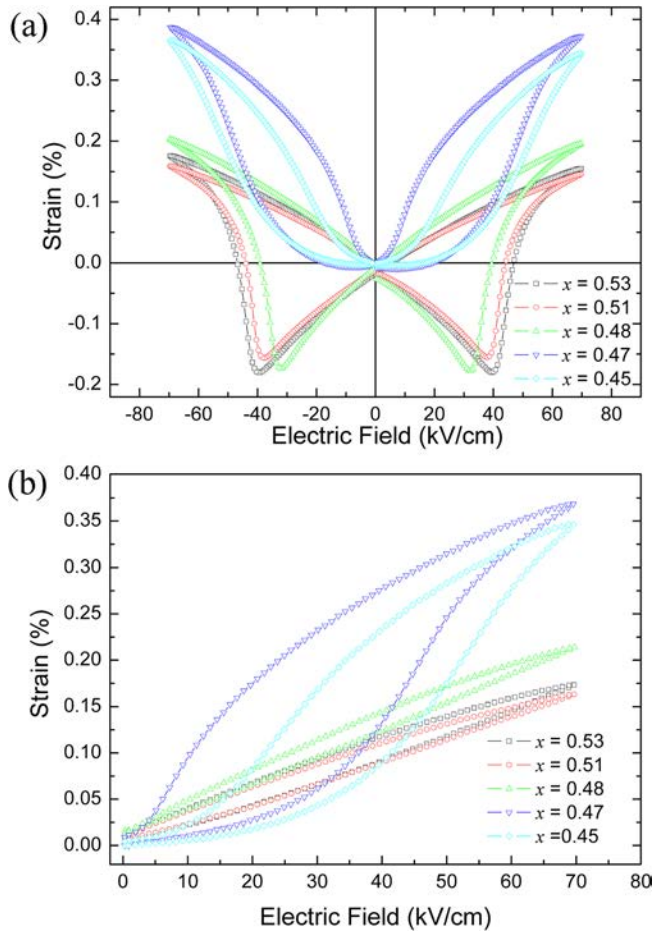

FIG. 4. (a) Bipolar and (b) unipolar strain curves vs. E-field of BMT-xPT-0.1BZ with $0.45 \leq x \leq 0.53$.

becomes obviously constricted, showing an antiferroelectric character. As shown in Fig. 3(b), the P_r changes slightly in the upper range of PT content. It is 31.8 μC/cm^2 at the MPB composition. While x decreases to 0.47, the P_r suddenly reduces to 6.21 μC/cm^2. This is similar to the change of the composition dependence of coercive field (E_C). For the antiferroelectric-like loops, we will also use E_C to identify their ferroelectricity instead of transition field ($E_{A\text{-}F}$).[9] The E_C decreases dramatically from 33.4 kV/cm for the $x = 0.48$ to 8.3 kV/cm for the $x = 0.47$, which might be due to the fact that the phase transition from FE to AFE state.[14] It needs to note that the result of polarization agrees well with the XRD pattern for the composition of $x = 0.48$. The well maintained P_r of $x = 0.48$ indicates that the transition for R to T phase can be stabilized even after unloading electric field.

The bipolar and unipolar strain vs. electric field, $S(E)$, curves are plotted in Fig. 4. Agreeing to the above $P(E)$ loops, the compositions of BMT-xPT-0.1BZ with $x \geq 0.48$ exhibit an archetypal butterfly shape curve. However, the $S(E)$ curves of BMT-0.47PT-0.1BZ and BMT-0.45PT-0.1BZ, which are in the R phase, totally differ to the ferroelectric one: the negative part of the strain curve becomes flatter. This behavior could be attributed to the antiferroelectric order.[14,15] According to the non-zero coercive field and remnant polarization for the composition of $x \leq 0.47$, it could be supposed that they are in antiferroelectric phase mixed with ferroelectric phase. The antiferroelectric order profits the large strain near the MPB.[9,14] Corresponding to the total strains of the bipolar $S(E)$ curves, the maximum strain of the unipolar $S(E)$ reaches as high as 0.37% at the composition of $x = 0.47$, as shown in Fig. 4(b). It is known that the unipolar displacement is related to the extrinsic effect of domain switching and intrinsic piezoelectric effect. The hysteresis of unipolar strain is attributed to the non-180° domain switching.[4,14,16] The lower hysteresis of BMT-0.48PT-0.1BZ (9.4%) than that of BMT-PT38 (24%) (Ref. 4) indicates that the $BaZrO_3$ substitution could dramatically reduce the

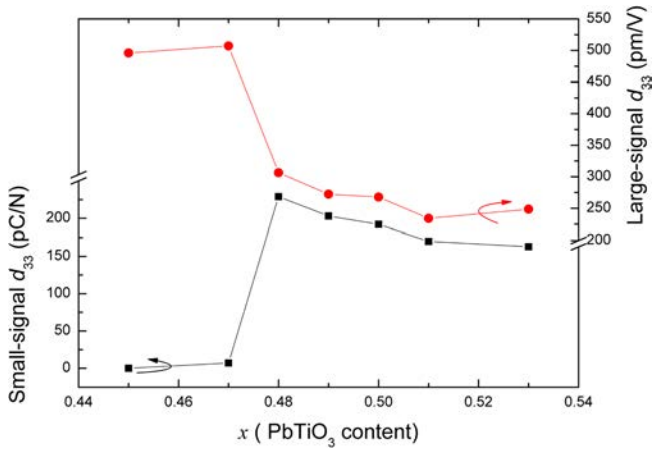

FIG. 5. Small and large-signal d_{33} for the BMT-xPT-0.1BZ with $0.45 \leq x \leq 0.53$.

extrinsic effect from the domain-switching, which is better for the application of actuator.

The piezoelectric properties as a function of PT content for the BMT-xPT-0.1BZ samples are shown in Fig. 5. For the compositions of $x \geq 0.48$, both small and large-signal d_{33} decrease with increasing amount of PT. The maximum of small-signal d_{33} value reaches 227 pC/N at the composition of $x = 0.48$. This value is similar to the MPB composition of BMT-PT fabricated with the precursor of $MgTiO_3$.[3] As x reduces to 0.47, the large-signal d_{33} reaches to the maximum value (520 pm/V), meanwhile the small-signal one diminishes nearly. This agrees well with the result of ferroelectric measurement that there is an FE-AFE phase transition at $x = 0.47$.

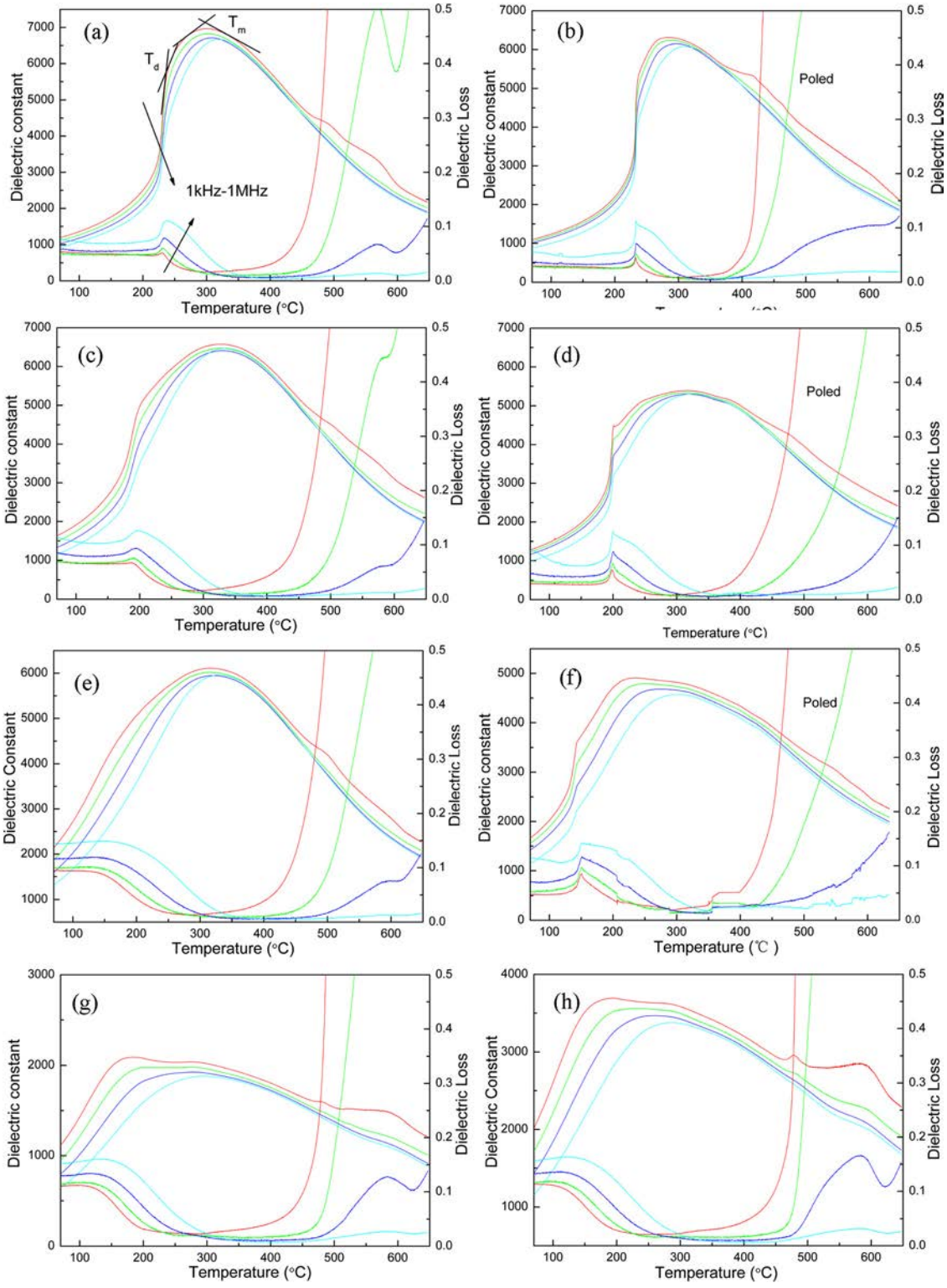

FIG. 6. Dielectric constant and loss as a function of temperature in the frequency range of 1 kHz to 1 MHz for the BMT-xPT-0.1BZ ($x = 0.53$, 0.5, 0.48, 0.47, and 0.45). (a), (c), (e), (g), and (h) are data for the unpoled ceramics, while (b), (d), and (f) are data for the poled ceramics.

In order to utilize the high temperature application of piezoelectric materials, not only the Curie temperature but also the depoling temperature are significant. Fig. 6 shows the temperature dependence of dielectric permittivity measured at different frequencies (1 kHz-1 MHz) on the unpoled and poled BMT-xPT-0.1BZ ceramics ($x = 0.45$, 0.47, 0.48, 0.50, and 0.53). Both unpoled and poled specimens display two dielectric anomalies for the ceramics with $x \geq 0.48$. The temperature of the first anomaly is the depolarization temperature (T_d), which corresponds to the transition from the ferroelectric state to antiferroelectric one (FE-AFE). The temperature at which the dielectric constant reaches the maximum value (T_m) corresponds to the antiferroelectric-paraelectric (AFE-PE) transition.[17] It can be seen that both FE-AFE and AFE-PE phase transitions occur in a wide temperature range, and the dielectric peaks at T_d and T_m (Fig. 6(a)) are frequency dependence, which indicates that the BMT-xPT-0.1BZ possesses a relaxor character. Especially, the FE-AFE phase transition temperature is widened, and the relaxor property is enhanced with the decrease in the PT content. This relaxor property may derive from the BMT-PT system.[3,18] For the compositions of BMT-PT in the R phase, microdomain structures related to strong frequency dispersion are mainly observed.[3] It is similar to the BNT-BT where the nanodomains appear at the MPB composition and their volumes increase with increasing $BaTiO_3$ content.[19,20] With increasing temperature, the nanodomains increase also.[21] The increase in the volume of nanodomains broadens the FE-AFE phase transition temperature range. Therefore, the similar dielectric properties could hypothesize that the BMT-xPT-0.1BZ behaves a similar domain structure to the BNT-BT.

For the poled ceramics, both the dielectric constant and dielectric loss vary sharply at T_d, as shown in Figs. 6(b), 6(d), and 6(f). We can identify the T_d according to the dielectric loss on poled pellet. The T_d and T_m are about 140 °C and 300 °C for the BMT-0.48PT-0.1BZ, respectively. The T_m is lower than that of the BMT-PT system.[3] It has been known that the high T_C of $PbTiO_3$-Bi$Me$$O_3$ is associated with the strong hybridization between the Pb/Bi and O.[22] The replacement of ionic Ba^{2+} to Pb^{2+}/Bi^{3+} would weaken such hybridization, resulting in the decrease in the T_m. It is the same with the ionic Sr-substitution in the Bi(Ni,Ti)O_3-PT system.[23] Even through the Curie temperature is reduced, the dielectric loss can be much reduced at high temperature up to 400 °C. The addition of $BaZrO_3$ benefits in the improvement of resistivity of BMT-PT.[3,4]

In order to further confirm the exact phase transition of FE-AFE suggested from the results of dielectric property, the temperature dependence of $P(E)$ and $S(E)$ curves for the BMT-0.48PT-0.1BZ were employed. As shown in Fig. 7(a), for the BMT-0.48PT-0.1BZ, the P-E loops display that the P_{max} of the sample is invariable, but the P_r slightly decreases as a function of temperature below 130 °C. When the temperature is above 145 °C, the hysteresis loop becomes "pinched" similar to that of antiferroelectric materials.[16,19] With further increase in temperature, the P_r keeps continuing to weaken. The antiferroelectric order is enhanced, while the ferroelectric order is depressed. However, the P_r is still non-zero at 160 °C, when the electric field is completely unloaded. It suggests that the sample possesses both ferroelectric and antiferroelectric orders above the T_d. Similar to the BNT-BT, the broadened temperature range of phase transition from the FE to AFE state could be associated with the coexistence of ferroelectric and antiferroelectric domains.[17,19,21] It needs to note that the FE-AFE phase transition manifested by the temperature dependent $P(E)$ loops is in a good agreement with the result of dielectric constant on the poled pellet. Therefore, the phase between the T_d and T_m could be concluded to be antiferroelectric-relaxor (AFE-relaxor), which was suggested in the lead-free BNT-BT system.[19–21,24] It has been known that the AFE-relaxor phase in the BNT-BT is caused by the fact that the nano-AFE $P4bm$ phase embeds in the ferroelectric $R3c$ matrix. The existence of AFE $P4bm$ lowers the T_d and can present at room temperature at the MPB of BNT-BT.[19] The orthorhombic structure of Bi($Mg_{1/2}Ti_{1/2}$)O_3 ($Pnnm$) analogous to $PbZrO_3$ may also attribute to the property of the AFE-relaxor in the BMT-PT based system.[10]

From the dielectric and ferroelectric properties as a function of composition and temperature and XRD data, a composition and temperature phase diagram could be designed for the poled BMT-xPT-0.1BZ ceramics with $0.45 \leq x \leq 0.53$ (Fig. 8). The phases at $T < T_d$ and $T > T_m$ are classical ferroelectric phase and cubic phase,

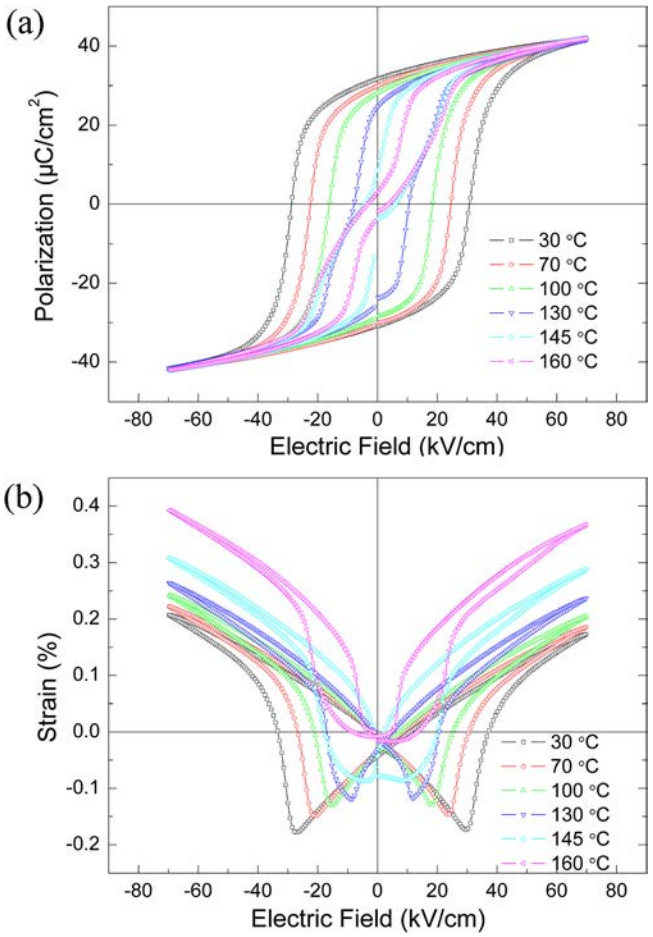

FIG. 7. Temperature dependence of (a) $P(E)$ and (b) $S(E)$ curves for the BMT-0.48PT-0.1BZ.

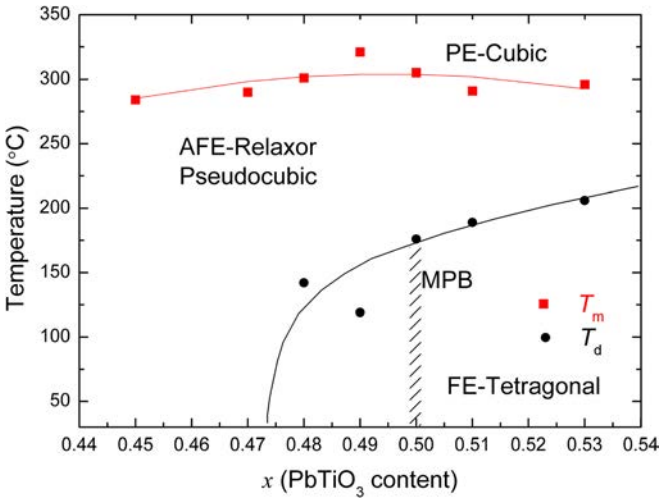

FIG. 8. Phase diagram of BMT-xPT-0.1BZ.

respectively. The phase in $T_d < T < T_m$ is thought to be the AFE-relaxor similar to BNT-BT.[19–21] In the composition between the 0.48 and the MPB ($x = 0.50$), the AFE-relaxor phase can be transformed into the ferroelectric T phase by electric poling and stabilized below the T_d.

IV. CONCLUSIONS

The pure perovskite phase of BMT-xPT-0.1BZ can be fabricated by conventional solid reaction. The position of MPB composition is BMT-0.50PT-0.1BZ for the crushed unpoled ceramic powder. The substitution of $BaZrO_3$ reduces the E_C and improves the electric resistance at high temperature. With the addition of $BaZrO_3$, the AFE-relaxor is induced in the BMT-PT. For the BMT-0.48PT-0.1BZ, the phase transition temperatures of T_d and T_m are 140 °C and 300 °C, respectively. In the AFE-relaxor phase of BMT-0.47PT-0.1BZ, the unipolar strain is 0.37%, and the large signal d_{33} is 530 pm/V.

ACKNOWLEDGMENTS

This work was supported by National Natural Science Foundation of China (Grant Nos. 91022016, 21031005, and 50974105), the Fundamental Research Funds for the Central Universities, China (Grant No. FRF-TP-09-004B), the Foundation for the Author of National Excellent Doctoral Dissertation of PR China (Grant No. 201039), and Program for New Century Excellent Talents in University (NCET-11-0573).

[1]R. E. Eitel, C. A. Randall, T. R. Shrout, and P. W. Rehrig, Jpn. J. Appl. Phys. **40**, 5999 (2001).
[2]R. E. Eitel, C. A. Randall, T. R. Shrout, and S.-E. Park, Jpn. J. Appl. Phys. **41**, 2099 (2002).
[3]C. A. Randall, R. Eitel, B. Jones, and T. R. Shrout, J. Appl. Phys. **95**, 3633 (2004).
[4]J. Chen, X. Tan, W. Jo, and J. Rödel, J. Appl. Phys. **106**, 034109 (2009).
[5]S.-E. Park and T. R. Shrout, J. Appl. Phys. **82**, 1804 (1997).
[6]S.-T. Zhang, A. B. Kounga, E. Aubach, H. Ehrenberg, and J. Rödel, Appl. Phys. Lett. **91**, 112906 (2007).
[7]E. M. Sabolsky, S. Trolier-McKinstry, and G. L. Messing, J. Appl. Phys. **93**, 4072 (2003).
[8]S.-F. Liu, S.-E. Park, L. E. Cross, and T. R. Shrout, J. Appl. Phys. **92**, 461(2002).
[9]W. Y. Pan, C. Q. Dam, Q, M. Zhang, and L. E. Cross, J. Appl. Phys. **66**, 6014 (1989).
[10]D. D. Khalyavin, A. N. Salak, N. P. Vyshatko, A. B. Lopes, N. M. Olekhnovich, A. V. Pushkarev, I. I. Maroz, and Y. V. Radyush, Chem. Mater. **18**, 5104 (2006).
[11]S. Wada, K. Yamato, P. Pulpan, N. Kumada, B.-Y. Lee, T. Iijima, C. Moriyoshi, and Y. Kuroiwa, J. Appl. Phys. **108**, 094114 (2010).
[12]C. Xu, D. Lin, and K. W. Kwok, Solid State Sci. **10**, 934 (2008).
[13]Y. Hiruma, H. Nagata, and T. Takenaka, Jpn. J. Appl. Phys. **48**, 09KC08 (2009).
[14]S.-T. Zhang, A. B. Kounga, E. Aulbach, W. Jo, and T. Granzow, J. Appl. Phys. **103**, 034107 (2008).
[15]S.-T. Zhang, A. B. Kounga, E. Aulbach, W. Jo, and T. Granzow, J. Appl. Phys. **103**, 034108 (2008).
[16]I. Kerkamm, P. Hiller, T. Granzow, and J. Rödel, Acta Mater. **57**, 77 (2009).
[17]S.-T. Zhang, A. B. Kounga, E. Aulbach, and Y. Deng, J. Am. Ceram. Soc. **91**, 3950 (2008).
[18]Q. Zhang, Z. Li, F. Li, Z. Xu, and X. Yao, J. Am. Ceram. Soc. **93**, 3330 (2010).
[19]C. Ma, X. Tan, E. Dul'kin, and M. Roth, J. Appl. Phys. **108**, 104105 (2010).
[20]C. Ma and X. Tan, Solid State Commun. **150**, 1497 (2010).
[21]C. Ma and X. Tan, J. Am. Ceram. Soc. **94**, 4040 (2011).
[22]M. Yashima, K. Omoto, J. Chen, H. Kato, and X. R. Xing, Chem. Mater. **23**, 3135 (2011).
[23]H. Kang, J. Chen, L. Liu, C. Hu, L. Fang, and X. R. Xing, J. Am. Ceram. Soc. **95**, 1170 (2012).
[24]S.-T. Zhang, A. B. Kounga, W. Jo, C. Jamin, K. Seifert, T. Granzow, J. Rödel, and D. Damjanovic, Adv. Mater. **21**, 4716 (2009).